

AgentSense: LLMs Empower Generalizable and Explainable Web-Based Participatory Urban Sensing

Xusen Guo¹, Mingxing Peng¹, Xixuan Hao¹, Xingchen Zou¹,

Qiongyan Wang¹, Sijie Ruan², Yuxuan Liang¹ [†]

¹The Hong Kong University of Science and Technology (Guangzhou), Guangzhou, China

²Beijing Institute of Technology, Beijing, China

{xguo796,mpeng060,xhao390,xzou428,qwang650}@connect.hkust-gz.edu.cn

sjruan@bit.edu.cn,yuxliang@outlook.com

Abstract

Web-based participatory urban sensing has emerged as a vital approach for modern urban management by leveraging mobile individuals as distributed sensors. However, existing urban sensing systems struggle with limited generalization across diverse urban scenarios and poor interpretability in decision-making. In this work, we introduce **AgentSense**, a hybrid, training-free framework that integrates large language models (LLMs) into participatory urban sensing through a multi-agent evolution system. AgentSense initially employs classical planner to generate baseline solutions and then iteratively refines them to adapt sensing task assignments to dynamic urban conditions and heterogeneous worker preferences, while producing natural language explanations that enhance transparency and trust. Extensive experiments across two large-scale mobility datasets and seven types of dynamic disturbances demonstrate that AgentSense offers distinct advantages in adaptivity and explainability over traditional methods. Furthermore, compared to single-agent LLM baselines, our approach outperforms in both performance and robustness, while delivering more reasonable and transparent explanations. These results position AgentSense as a significant advancement towards deploying adaptive and explainable urban sensing systems on the web.

Keywords

Web Mining, Participatory Urban Sensing, LLM, Agentic AI

1 Introduction

The Web has become a fundamental infrastructure for urban sensing, enabling large-scale data collection, coordination, and interaction between citizens, devices, and city systems. Web-based platforms and mobile applications allow individuals, such as commuters, ride-hailing drivers, and couriers, to act as distributed sensors, continuously contributing spatio-temporal data through their daily activities. This paradigm, often termed **Web-based Participatory Urban Sensing (WPUS)** [4, 18, 33], transforms the Web from a medium of information sharing into an active channel for real-time urban intelligence, powering applications in traffic monitoring [8, 38, 42], environmental sensing [13, 20, 47], and infrastructure management [50, 52]. Compared with fixed sensor networks, which are costly and static, web-enabled crowdsensing offers scalability, adaptability, and operational efficiency, making it a cornerstone for responsive, data-driven smart city services [17, 36].

[†]Corresponding Author. Email: yuxliang@outlook.com.

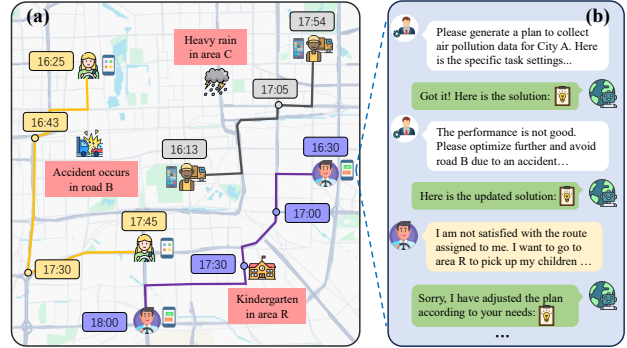


Figure 1: (a): Web-based urban sensing under dynamic conditions. (b): AgentSense adaptively refines baseline solutions in response to evolving requirements.

Early research on WPUS has made progress through optimization-based task allocation [13, 18, 19] and learning-driven approaches [41]. The first class formulates the sensing assignment as a combinatorial problem under budget and data coverage constraints, while the latter introduces heuristics or reinforcement learning to improve scalability and adaptivity. These methods have proven effective in specific settings, but they remain largely limited to static assumptions and narrowly defined task environments. Despite progress, two critical challenges persist: i) **Context-Aware Generalization** is limited. Urban environments are inherently dynamic, shaped by real-time factors such as traffic, weather, and evolving worker availability (see (Figure 1(a))). Most systems cannot flexibly re-optimize task assignments under such disturbances [34, 35], and they often assume homogeneous worker behavior [6, 18]. Consequently, resources are used inefficiently, task distribution becomes inequitable, and models trained in one city fail to generalize to new contexts without costly retraining [7, 41]. ii) **Transparent Interpretability** also remains unresolved. Current methods [18, 41, 45] typically act as black boxes, offering no rationale for task reassignments or route changes. This lack of explanation undermines transparency and trust, particularly in safety-critical scenarios such as emergency response or public safety monitoring.

Recent advances in Large language models (LLMs) [21, 24, 49] present new opportunities to overcome these challenges. For context-aware generalization, LLMs have demonstrated strong reasoning in complex, dynamic environments and robust zero-shot transfer across tasks and domains [1, 22]. These capabilities make them

well-suited to integrate real-time urban disturbances with heterogeneous worker preferences, enabling adaptive and transferable task assignments. For transparent interpretability, LLMs naturally generate step-by-step reasoning and human-readable feedback, offering a pathway to explain why tasks are reassigned or routes adjusted, thereby improving trust in system decisions. However, directly applying LLMs to participatory urban sensing still remains infeasible, as the task assignment problem in WPUS is NP-hard, requiring combinatorial optimization beyond their generative capacity.

To harness the complementary strengths of both worlds, we introduce **AgentSense**, a hybrid and training-free framework that integrates LLMs into WPUS through a *multi-agent* loop. Our AgentSense *combines the feasibility guarantees of classical planners with the generalizability and interpretability enabled by LLM-powered collaboration*. First, an initial solution is first generated by an optimization planner to satisfy fundamental constraints such as budget and coverage. This solution is then iteratively refined by three synergistic agents: a **Solver Agent** that proposes updates under dynamic disturbances, an **Eval Agent** that assesses solutions with quantitative metrics (such as coverage, budget compliance, and fairness) and structured feedback, and a **Memory Agent** that accumulates reusable meta-operations to accelerate convergence. As depicted in Figure 1(b), this design innovatively transforms WPUS into an interactive web-based platform that continuously adapts task assignments to evolving conditions while providing transparent explanations to participants and stakeholders. In summary, our contributions are fourfold:

- **Dynamic and Personalized Task Assignment:** We propose AgentSense, a framework that adapts to real-time urban dynamics and heterogeneous participant preferences, enabling efficient, fair, and personalized task allocations.
- **Zero-Shot Generalization Across Tasks:** Leveraging the zero-shot capabilities of LLMs, AgentSense generalizes across diverse urban sensing tasks and environments without retraining, supporting rapid deployment in new scenarios.
- **Transparency and Interpretability:** AgentSense enhances explainability by generating step-by-step refinements and natural language feedback, thereby improving transparency and fostering trust in urban management applications.
- **Extensive Experimental Validation:** We conduct comprehensive experiments on two large-scale mobility datasets across seven types of disturbances, demonstrating that AgentSense consistently outperforms traditional methods in adaptivity and exceeds single-agent LLMs in both effectiveness and robustness.

2 Preliminary

2.1 Formulation

Definition 1 (Urban Sensing Problem) The urban sensing problem involves recruiting a group of participants (or termed workers) and assigning tasks to maximize the coverage of data collected within a specified spatial-temporal region, subject to a given budget. Following work [18], the problem can be formulated as:

$$\max \mathcal{J}(D), \text{ s.t. } \left\{ D = \sum_{i \in P} D_i, \sum_{i \in P} r_i \leq B \right\}, \quad (1)$$

where P is the set of recruited participants, D_i is the data collected by the sensing tasks assigned to participant i , r_i is the rewards allocated to participant i , and B is the total budget. The objective $\mathcal{J}(D)$ aims to maximize the overall data coverage, with each task defined as a location-time cell within a discretized city grid.

Definition 2 (Data Coverage) We define the measurement of data coverage based on a hierarchical entropy-based objective function $\mathcal{J}(D)$ proposed in [18]. The objective function is formulated as:

$$\mathcal{J}(D) = \alpha E(D) + (1 - \alpha) \log_2 Q(D), \quad (2)$$

where $E(D)$ represents the hierarchical entropy of the collected data D , which captures the balance of data at various spatial and temporal granularities, and $Q(D)$ is the total amount of collected data. The parameter α adjusts the relative importance between the balance of the data distribution and the total quantity of data.

Definition 3 (Adaptive Urban Sensing Problem) The adaptive urban sensing builds upon traditional approaches by incorporating real-time disturbances that may originate from environmental factors, participant-specific constraints, or system-level variations (e.g., road closures, adverse weather, or budget changes). The objective is to refine an initial urban sensing solution in response to these dynamic disturbances, ensuring feasibility and performance under changing conditions. Formally, the problem is defined as:

$$\max \mathcal{J}(D(\delta), S_0), \text{ s.t. } \left\{ D(\delta) = \sum_{i \in P(\delta)} D_i(\delta), \sum_{i \in P(\delta)} r_i \leq B(\delta) \right\},$$

where S_0 represents the initial solution, δ denotes the disturbances or changes applied to the initial problem, and $D(\delta)$, $P(\delta)$, $B(\delta)$ are the total data collected, the participant candidates, and the total budget after the disturbance, respectively.

2.2 Related Work

2.2.1 Participatory and Mobility-Driven Urban Sensing. Participatory urban sensing has become a cornerstone of smart city research, enabling fine-grained monitoring of environmental conditions [13, 20], transportation systems [38, 42], and urban infrastructure [50, 52], etc. Recent studies have mainly focused on two paradigms: *crowd-based human mobility sensing* and *vehicle-based drive-by sensing*. The former treats humans as mobile sensors, where participants contribute GPS traces [30], noise levels [53], or air quality data [27] during daily commutes. However, as noted in [18], human mobility is inherently skewed and uncertain, often leading to redundancy in popular areas while leaving peripheral regions under-sampled. To mitigate this imbalance, prior work has introduced entropy-driven objectives and graph-based task allocation methods under budget constraints [18, 39, 41]. In parallel, *drive-by sensing* leverages vehicles such as taxis, buses, or drones equipped with sensors to provide broader and more systematic coverage [2, 19, 29]. While this approach offers improved reliability, its effectiveness is constrained by fixed mobility patterns, leading to route clustering and persistent blind spots in areas not served by the fleet [10, 23, 44]. Despite these strengths, both paradigms typically assume static mobility and lack mechanisms to adapt to dynamic real-world disturbances. In contrast, our AgentSense leverages LLM-driven evolution framework to continuously updates task plans, dynamically adapting to real-time changes.

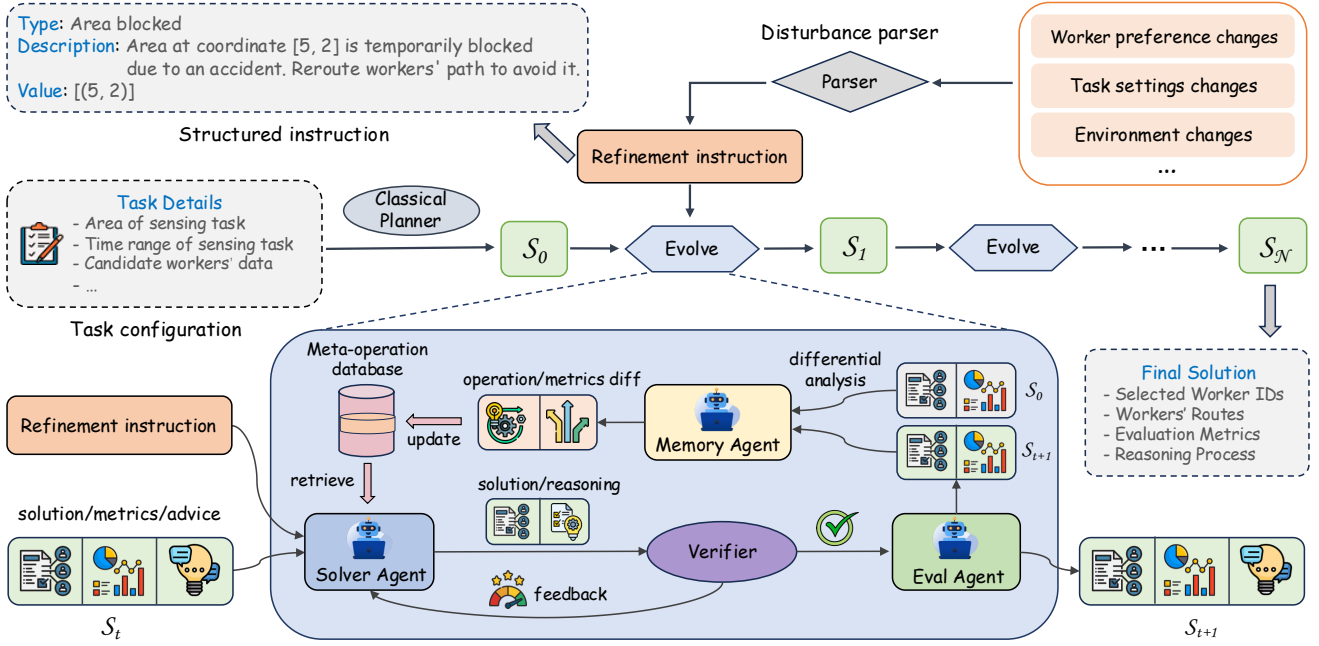


Figure 2: The AgentSense framework for iterative refinement of urban sensing task solution.

2.2.2 Large Language Models for Urban Computing. LLMs have made significant progress in recent years, demonstrating strong capabilities in reasoning [9, 21], instruction following [32, 49], and multi-agent collaboration [12, 14, 24, 37] across a wide range of domains [3, 5, 11, 31, 43, 51]. Their strong capacity for natural language understanding, coupled with their alignment to human preferences, makes LLMs particularly suitable for urban applications that require translating human intent into system-level actions. Recent research has begun to explore this potential within urban contexts [15, 25, 26, 28, 55]. In participatory planning, LLM agents can serve as both "planner" and "resident," synthesizing diverse stakeholder preferences into executable land-use strategies that outperform rule-based baselines and even human experts on service accessibility and ecological indicators [54]. In the mobility domain, LLM-driven agents generate explainable, habit-aware daily trajectories that closely match real-world distributions and remain robust under disruptions like pandemics [40]. At the city scale, OpenCity [46] scales LLM agent simulations to tens of thousands of individuals through prompt optimization and system-level acceleration, enabling high-fidelity modeling of urban dynamics and counterfactual policy evaluation. Together, these advances highlight that urban contexts offers a particularly suitable ground for LLMs. Building on this perspective, we introduce AgentSense, a LLM-based multi-agent framework for refining and adapting urban sensing plans under real-world disturbances.

3 Methodology

3.1 Overview

AgentSense is designed to adaptively handle urban sensing tasks in dynamic environments. As shown in Figure 2, it follows a dynamic

evolution workflow that begins with a classical planner generating an initial feasible schedule S_0 over the road graph or discretized spatial-temporal grid. This plan ensures basic constraint satisfaction (e.g., time windows, total budget) and serves as a reference for subsequent refinements. To adapt to evolving conditions such as user preference updates or external disruptions (e.g., blocked roads, adverse weather), the system employs two key components: (i) a *disturbance parser*, which converts unstructured dynamic signals into structured refinement instructions, and (ii) a *multi-agent refinement loop*, where an LLM-powered multi-agent system iteratively updates baseline solution. This process yields a refinement sequence $S_0 \rightarrow S_1 \rightarrow \dots \rightarrow S_N$, progressively improving solutions while preserving spatial-temporal feasibility and budget compliance.

3.2 Disturbance Parser

Web-sourced signals from the environment or user feedback are inherently unstructured and semantically diverse. To enable automated adaption over these signals, the disturbance parser leverages a large language model to translate them into structured refinement instructions. Each instruction is formatted as a dictionary with standardized fields *type*, *description*, and *value*. These structured messages precisely encode the scope and semantics of the required changes, enabling the downstream refinement process to operate over a unified, machine-interpretable interface.

3.3 Solver Agent

As the core component of the multi-agent refinement framework, *Solver Agent* is responsible for transforming a current solution S_t into an improved solution S_{t+1} in response to a structured refinement instruction δ . Its primary objective is to incorporate disturbances while preserving feasibility and optimizing key criteria such

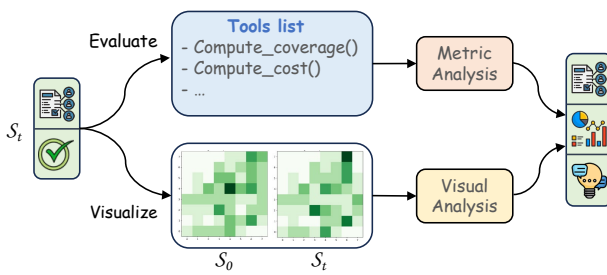


Figure 3: Eval Agent.

as spatial-temporal coverage and budget efficiency. To achieve this, the *Solver Agent* operates through an *iterative edit-and-verify* loop. At each step, it applies atomic and interpretable modifications (e.g., adding / removing workers, swapping task assignments), and verifies that the resulting plan remains valid. This fine-grained editing process ensures both transparency of reasoning and robustness.

While the *Solver Agent* orchestrates the refinement, it is supported by two auxiliary sources of guidance: evaluation feedback provided by the *Eval Agent* and historical meta-operations managed by the *Memory Agent*. These additional information allow the solver to prioritize promising adjustments, avoid redundant modifications, and accelerate convergence. Over successive refinements, the *Solver Agent* accumulates reusable heuristics, enabling more adaptive and efficient planning in dynamic urban sensing environments.

3.4 Eval Agent

The *Eval Agent* functions as a quality assessor and feedback generator within each refinement iteration. As illustrated in Figure 3, given a candidate solution S_t proposed by the *Solver Agent*, the *Eval Agent* evaluates its performance across multiple quantitative criteria with external function tools, including total data coverage and budget efficiency. Beyond numerical metrics, it also generates spatial-temporal diagnostics by visualizing coverage heatmaps for both the baseline solution S_0 and the refined solution S_t . This visual comparison helps identify gaps, or redundant routing patterns that can not be evident from metrics alone. The agent then composes its findings into a concise natural language report, which includes a ranked list of actionable suggestions. Examples include "reroute worker 46 to pass through the low-coverage top-left region" or "replace worker 2 with worker 5 to reduce cost while maintaining coverage." This structured feedback is passed to the *Solver Agent* to guide subsequent iterations, ensuring that the refinement process remains interpretable, goal-directed, and human-aligned.

3.5 Memory Agent

The *Memory Agent* enables experience-aware refinement by systematically recording and analyzing the solver's historical optimization trajectories. Given a baseline-refined solution pair (S_0, S_t) and their corresponding evaluation metrics $(\mathcal{M}_0, \mathcal{M}_t)$, the agent first computes the metric gap $\Delta\mathcal{M} = \mathcal{M}_t - \mathcal{M}_0$, which reflects the improvement or degradation induced by refinement. Next, the agent conducts a differential analysis between S_0 and S_t , extracting a set of interpretable atomic *meta-operations*:

$$\Delta S_t = \{o_1, o_2, \dots, o_n\}, \quad o_i \in O,$$

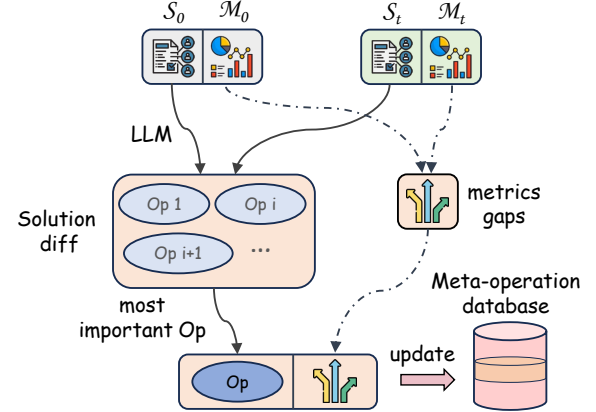


Figure 4: Memory Agent.

where O is the operation space (e.g., *reroute path segment* ζ of worker u , *add / remove worker* w , *replace task* i with j). Each operation o_i is then assigned an impact score

$$\phi(o_i | \Delta\mathcal{M}, C_t) \in \mathbb{R},$$

estimated by the LLM given the observed metric gap $\Delta\mathcal{M}$ and contextual metadata C_t (e.g., budget, region, disturbance type). The operation with the highest score is identified as a high-impact meta-operation:

$$o^* = \arg \max_{o_i \in \Delta S_t} \phi(o_i).$$

All high-impact operations, along with their context and associated $\Delta\mathcal{M}$, are stored in a persistent database \mathcal{D} . In subsequent refinement rounds, the *Solver Agent* queries this database with its current candidate operations $\Delta S_{t'}$, retrieving the top- k relevant past operations:

$$\text{Retrieve}(\Delta S_{t'}) = \text{Top-}k_{o \in \mathcal{D}} \sim(o, \Delta S_{t'}),$$

where $\sim(\cdot, \cdot)$ denotes an embedding-based similarity between operations. By leveraging these retrieved experiences, the solver learns from prior refinements, reuses successful strategies, and avoids repetitive failures. This memory-guided mechanism accelerates convergence and improves overall solution quality.

3.6 Comparison to Existing Arts

Table 1: Comparison of different paradigms in WPUS with different perspectives. ✓ / ✓ / ✗ indicates strong / moderate / lack of support.

Dimension	Classical	Learning-based	single LLMs	AgentSense
Solution quality	✓	✓	✓	✓
Efficiency	✓	✗	✗	✓
Explainability	✗	✗	✓	✓
zero-shot ability	✗	✗	✓	✓
Scalability	✓	✓	✗	✓

To better position our framework within the broader landscape, we compare **AgentSense** with existing paradigms in WPUS. As

summarized in Table 1, classical planners rely on explicit optimization rules, providing strong solution quality with high efficiency and scalability, yet their rule-based nature limits adaptability, resulting in poor explainability and a lack of zero-shot generalization. Learning-based approaches deliver high-quality solutions by leveraging data-driven modeling, but their dependence on training data reduces efficiency, limits scalability, and weakens interpretability. Single-agent LLMs, by contrast, offer explainability and zero-shot generalization through intrinsic reasoning ability, but often generate infeasible solutions and suffer from high computational costs in complex reasoning, which prevents scalability. By integrating classical planning with a multi-agent refinement loop, **AgentSense** combines structural reliability with LLM-driven adaptability, achieving consistently high solution quality while ensuring interpretability and generalization. Although its efficiency and scalability remain constrained by the computational burden of LLMs, AgentSense leverages baseline solutions to confine exploration within a feasible subspace, thereby achieving a balanced trade-off.

4 Experiments

In this section, we evaluate the performance of *AgentSense* across five key research questions:

- **RQ1:** How significantly does AgentSense improve upon strong single-agent LLM baselines across diverse urban sensing tasks?
- **RQ2:** Does better baseline planners lead to better performance?
- **RQ3:** How effectively does AgentSense adapt to diverse real-world disturbances while maintaining solution quality?
- **RQ4:** How do the *Eval Agent* and the *Memory Agent* contribute to overall efficiency and quality of the solution?
- **RQ5:** How does AgentSense improve upon single-agent LLM baselines in terms of explanation?

To answer these questions, we conduct extensive experiments across diverse task settings and disturbances.

4.1 Experimental Setup

4.1.1 Datasets. We conduct experiments on two large-scale real-world mobility datasets, T-Drive [48] and Grab-Posisi [16], which span diverse urban regions and mobility patterns. T-Drive contains GPS traces over ten thousands taxis in Beijing over a week in 2008, offering rich spatiotemporal signals for large-scale sensing. Grab-Posisi, released by Grab, records high-frequency positional data from ride-hailing drivers across cities like Jakarta, enabling fine-grained analysis in dense urban settings.

To evaluate our framework under different complexities, we define three configurations (*Small*, *Medium*, and *Large*) for each dataset, as summarized in Table 2. In the *Small* T-Drive setting, for instance, the city is discretized into an $8 \times 8 \times 8$ spatial-temporal sensing grid (15-minute intervals over a 2-hour horizon), with each cell corresponds to a distinct urban sensing task. We sample 20 workers and allocate a total budget of 40, which specifies the maximum cumulative rewards distributed across workers. Following prior work [18, 41], workers are assumed to move at constant speed in free space with a normalized reward of 1.0 per time step. Across all settings, the sensing task time interval is fixed at 15 minutes for T-Drive and 5 minutes for Grab-Posisi. To ensure robustness, we random generate 20 task instances for each setting in each dataset.

Table 2: Details of datasets.

Dataset	Scale	Workers	Grid Size	# Regions	Total Budget	Horizon (min)
T-Drive	Small	20	8×8	64	40	120
	Medium	40	16×16	256	60	240
	Large	60	32×32	1024	100	360
Grab-Posisi	Small	15	8×4	32	40	40
	Medium	30	16×8	128	60	80
	Large	45	32×16	512	100	160

4.1.2 Evaluation Metrics. To quantitatively assess the performance of AgentSense and baseline models, we adopt three evaluation metrics that capture both effectiveness and efficiency. **SR** (Success Rate) denotes the proportion of runs (out of 20 independent trials) where the refined solution achieves a valid improvement over the baseline within at most 10 iterations. **AIR** (Average Improvement Rate) measures the relative improvement in the main objective function (Equation 2, with $\alpha = 0.5$ by default) compared to the baseline solution. **ANI** (Average Number of iterations) records the average number of refinement steps required to obtain a valid improvement, reflecting the convergence speed of the refinement process. Finally, **ACS** (Average Cost Savings) quantifies the reduction in budget usage, where negative values correspond to a cost increase.

4.2 Overall Performance (RQ1)

To underscore the advantages of AgentSense over single-agent LLM baselines, Table 3 reports a comparative evaluation on two datasets across all three task settings. As expected, all models exhibit notable performance drops from the *Small* to the *Large* setting, validating the effectiveness of our task hierarchy in reflecting increasing complexity. Furthermore, performance trends remain consistent across both datasets, indicating strong generalization of LLM-based approaches to diverse urban sensing task configurations.

Delving deeper, single-agent LLMs exhibit distinct trade-offs between feasibility and performance. Advanced models like GPT-4.1 and Claude-3.7 achieve high AIR in the *Small* setting (e.g., 1.352% and 1.165% on T-Drive), but their SR declines sharply to 30.0% and 45.0% in the *Large* setting due to frequent budget violations, suggesting an overly aggressive optimization strategy. In contrast, models such as GPT-3.5-turbo and DeepSeek-R1 adopt more conservative refinements, yielding higher SR but lower AIR. AgentSense, by comparison, achieves both high feasibility and strong improvement across all settings, for instance, attaining 100.0% SR and 1.622% AIR on Grab-Posisi *Small*, and maintaining 95.0% SR and 0.983% AIR even on T-Drive *Large*. These results highlight the benefits of AgentSense's multi-agent iterative refinement, which balances performance gains with constraint adherence through cyclic verification, enabling robust and consistent enhancements beyond single-agent paradigms.

4.3 Performance on Different Baselines (RQ2)

In this section, we investigate whether stronger baseline planners lead to better overall performance when combined with AgentSense. To this end, we evaluate AgentSense on 20 problem instances from the T-Drive dataset with six baseline algorithms: *Random* (RN), *Task Value Priority Greedy* (TVPG), *Task Cost Priority Greedy* (TCPG), *Multi-Start Simulated Annealing* (MSA), *Multi-Start Simulated Annealing with Greedy Initialization* (MSAGI), and an advanced *Graph-based Dynamic Programming* (GraphDP) method. The first five are

Table 3: Comparison of single-agent LLMs and AgentSense on the T-Drive and Grab-Posisi problem sets across three task settings. SR denotes the success rate over 20 trials, and AIR represents the average improvement rate of the objective value.

Type	Model	T-Drive						Grab-Posisi					
		Small		Medium		Large		Small		Medium		Large	
		SR	AIR	SR	AIR	SR	AIR	SR	AIR	SR	AIR	SR	AIR
<i>Proprietary LLMs</i>													
SA	gpt-3.5-turbo-0125	95.0	0.894	90.0	0.202	70.0	-0.541	95.0	0.934	85.0	0.185	75.0	-0.453
	gpt-4.1-2025-04-14	70.0	1.352	55.0	0.982	30.0	0.091	75.0	1.503	60.0	0.880	50.0	0.105
	gemini-2.0-flash	100.0	0.904	85.0	0.320	65.0	0.084	95.0	0.864	90.0	0.240	65.0	0.232
	claude-3-7-sonnet	65.0	1.165	55.0	1.059	45.0	0.722	70.0	1.244	55.0	1.123	50.0	0.504
	claude-3-5-sonnet	65.0	0.620	50.0	0.455	25.0	0.246	65.0	0.598	55.0	0.401	35.0	0.277
<i>Open-Source LLMs</i>													
SA	deepseek-r1	100.0	0.520	85.0	-0.183	70.0	-0.677	100.0	0.497	90.0	0.092	75.0	-0.744
	qwen3-235b-a22b	100.0	0.433	70.0	0.370	55.0	0.012	95.0	0.465	70.0	0.401	50.0	-0.043
	Llama-3-70B-instruct	70.0	1.208	85.0	0.314	65.0	0.087	75.0	0.993	80.0	0.287	55.0	0.094
MA	AgentSense	100.0	1.545	100.0	1.162	95.0	0.983	100.0	1.622	100.0	1.248	100.0	0.648

Table 4: Performance of AgentSense under different baseline planners across three task settings on T-Drive problem sets.

Baselines	Small				Medium				Large			
	Base Obj. ↑	Final Obj. ↑	AIR (%) ↑	Tokens ($\times 10^5$) ↓	Base Obj. ↑	Final Obj. ↑	AIR (%) ↑	Tokens ($\times 10^5$) ↓	Base Obj. ↑	Final Obj. ↑	AIR (%) ↑	Tokens ($\times 10^5$) ↓
RN	4.505	4.630	2.775	1.620	4.706	4.784	1.657	2.770	5.029	5.221	3.818	5.733
TVPG	4.565	4.632	1.468	1.719	4.761	4.811	1.050	3.013	5.602	5.662	1.071	6.140
TCPG	4.588	4.628	0.872	1.968	5.118	5.178	1.172	3.207	5.544	5.617	1.317	6.505
MSA	4.662	4.674	0.257	2.356	5.086	5.136	0.983	4.873	5.631	5.677	0.817	6.953
MSAGI	4.702	4.713	0.234	2.524	5.090	5.101	0.212	4.860	5.682	5.699	0.299	7.834
GraphDP [18]	4.780	4.788	0.167	2.894	5.205	5.254	0.365	4.797	5.701	5.708	0.175	8.270

sourced from [41], while the GraphDP method is implemented according to [18]. Detailed introduction are provided in Appendix A.

Results in Table 4 shows that AgentSense consistently improves all baselines across all three settings. However, the degree of improvement is inversely related to baseline strength. For instance, AgentSense improves the *RN* baseline by 2.775% in the *Small* setting and 3.818% in the *Large* setting, whereas gains on the more powerful baseline *GraphDP* are minimal (0.167% and 0.175% respectively) and come with much higher token costs (2.894×10^5 in *Small* and 8.270×10^5 in *Large*). This pattern reflects diminishing returns: as baseline quality approaches near-optimality, the space for refinement shrinks while the computational overhead of marginal improvements increases. Overall, weaker baselines such as *TVPG* and *TCPG* yield more cost-effective improvements with our framework, suggesting that it is often more efficient to start from a moderately strong baseline and leverage AgentSense for enhancement rather than beginning with an already highly optimized solution. In this paper, *TVPG* is adopted as the default planner.

4.4 Performance on Disturbances (RQ3)

We evaluates AgentSense under seven types of dynamic disturbances commonly encountered in WPUS:

- **Budget change:** the budget dynamically increases / decreases.
- **Area blocked:** certain regions become temporarily inaccessible.
- **Priority area:** importance regions require priority coverage.
- **Mid-path visit:** workers require additional mid-path visiting.

- **Worker unavailable:** one or more workers drop out.
- **New worker available:** additional workers join the task.
- **Bad weather:** adverse weather reduce worker mobility.

While these seven cases are used for evaluation, AgentSense is not restricted to them. With suitable prompt design, the framework can flexibly accommodate other real-world disturbances.

Table 5 shows that AgentSense demonstrates strong robustness across all disturbance types. In the *Small* and *Medium* settings, it consistently achieves perfect success rates (SR = 100.0%) and converges within relatively few iterations. The refined solutions generally remain feasible with negligible efficiency loss. For instance, under *Area blocked*, the performance impact is minimal (AIR = -0.12%, ACS = 0.10 in *Medium*), and both metrics stay close to zero in the *Large* setting, indicating that AgentSense can reliably adapt baseline plans into high-quality, constraint-satisfying solutions. In the *Large* setting, disturbance adaption becomes more challenging, reflected in slightly reduced success rates (e.g., SR = 90.0% for *mid-path visiting* and 95.0%). Nevertheless, the system still converges after several refinement rounds and maintains feasible solutions. Among all disturbances, *bad weather* exerts the strongest negative influence on AIR (e.g., -28.503% in *Small*, -44.292% in *Large*), since reduced worker mobility inherently limits achievable coverage. Even in this case, AgentSense preserves budget feasibility and leverages dynamic reallocation to mitigate performance degradation as much as possible.

Table 5: Performance of AgentSense under different disturbances on 20 T-Drive problems. Metrics include SR (Success Rate), AIR (Average Improvement Rate), ANI (Average Number of Iterations), and ACS (Average Cost Savings).

Disturbances	Small				Medium				Large			
	SR (%) ↑	ANI ↓	AIR (%) ↑	ACS ↑	SR (%) ↑	ANI ↓	AIR (%) ↑	ACS ↑	SR (%) ↑	ANI ↓	AIR (%) ↑	ACS ↑
Budget change (increase)	100.0	5.6	5.855	–	100.0	6.6	6.424	–	100.0	8.5	3.227	–
Area blocked	100.0	7.4	-0.551	-0.10	100.0	7.2	-0.121	0.10	95.0	8.3	0.000	0.00
Priority area	100.0	6.1	-0.882	0.00	100.0	7.9	-0.320	0.20	100.0	8.9	-0.182	-0.10
Mid-path visiting	100.0	7.3	-0.667	0.10	95.0	8.5	-0.783	-0.26	90.0	9.3	-1.260	3.00
Worker unavailable	100.0	4.4	-1.220	2.00	100.0	6.7	-0.967	2.00	100.0	7.7	-0.933	-0.75
New worker available	100.0	5.0	0.238	-1.00	100.0	6.6	0.372	-1.00	100.0	8.4	1.889	1.50
Bad weather	100.0	6.3	-28.503	0.00	100.0	7.1	-34.550	2.00	95.0	9.7	-44.292	1.95

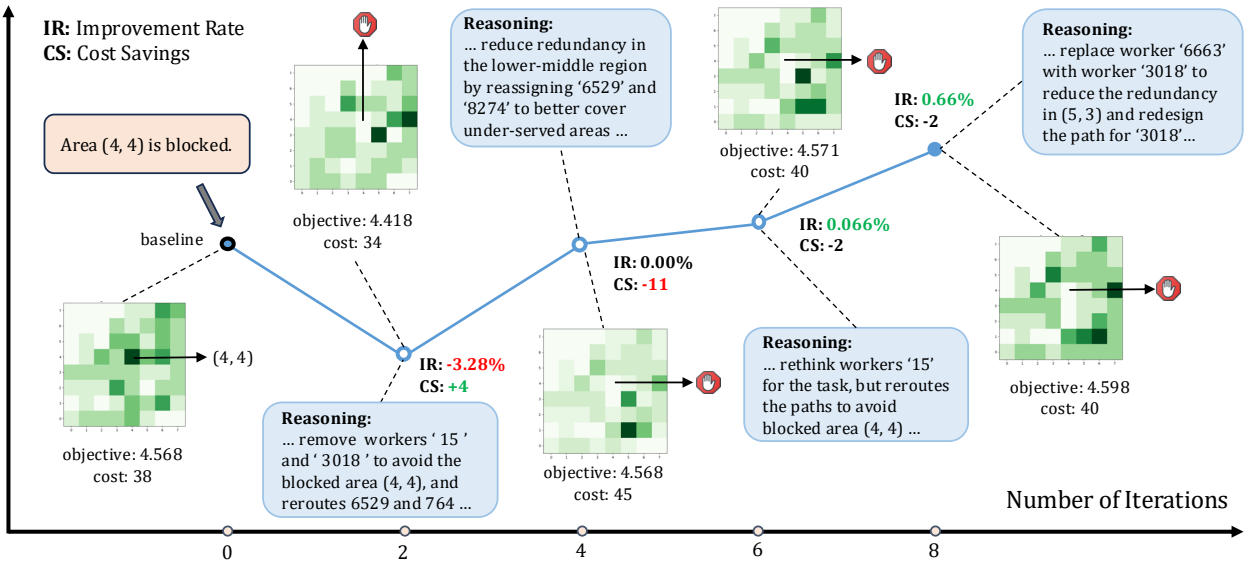


Figure 5: Iterative improvement process for disturbance "Area blocked (4, 4)".

To better illustrate the refinement process, Figure 5 presents the optimization trajectory under an *Area blocked* disturbance in the T-Drive *Small* setting. Starting from an infeasible baseline, AgentSense incrementally reassigned workers and reroutes paths, with each step explained through natural language reasoning. The first adjustment avoided the blocked area but reduced data coverage, whereas later refinements improved coverage at the expense of sharply increased costs that exceeded the budget. After several corrections, the system converged to a feasible solution with higher coverage and budget compliance. This case highlights how iterative refinement enables AgentSense to recover from infeasibility and balance competing objectives under disturbances. Beyond this example, we further provide two additional results in Figure 6, illustrating AgentSense’s adaptability to a *Mid-path visiting* and a *Priority area* disturbances. We highlight the significant changes in the routes by red arrows. Together, these cases demonstrate the framework’s robustness in handling diverse real-world disturbances.

4.5 Ablation Studies (RQ4)

In this section, we analyze how the vision module of the *Eval Agent* and the structured memory maintained by the *Memory Agent* affect

the overall performance. Figure 7 reports the ablation results, where the left panel shows the performance metric *AIR* and the right panel presents the convergence efficiency metric *ANI*. The variant *Ours w/ History* replaces the *Memory Agent* with direct reuse of prior solutions as static references.

The results demonstrate that disabling either the vision module or the *Memory Agent* leads to notable performance degradation, evidenced by reduced *AIR* and slower convergence (higher *ANI*). This underscores the critical role of these components, since vision module enables the *Eval Agent* to reason over coverage distributions from a global perspective, facilitating faster identification of under-served regions and more informed refinements. Concurrently, the *Memory Agent* leverages meta-operation-based memories to provide structured, transferable priors, effectively guiding the refinement process and minimizing redundant exploration. Additionally, we observe that directly reusing historical plans (*Ours w/ History*) performs even worse than the no-memory baseline. This likely stems from the fact that raw solutions are structurally complex, making them hard for LLMs to interpret. Moreover, they

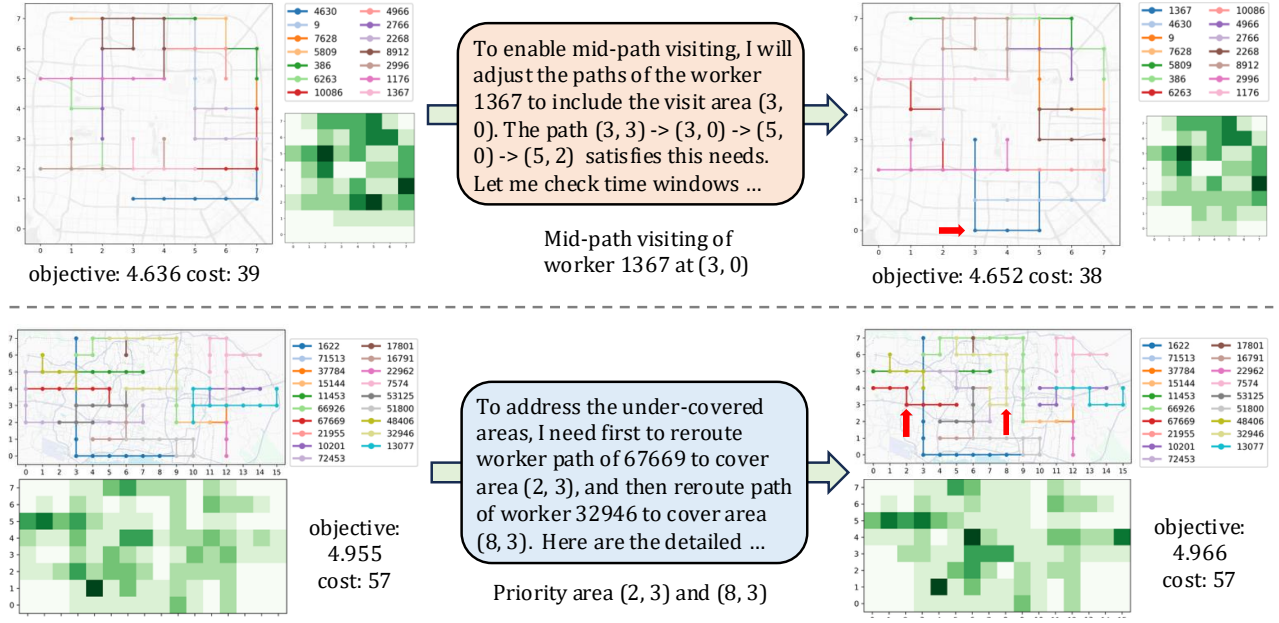


Figure 6: Adaptation results under different disturbances: (top) *Mid-path visiting* in T-Drive Small setting, and (bottom) *Priority area* in Grab-Posisi Medium setting. Significant route changes are highlighted with red arrows.

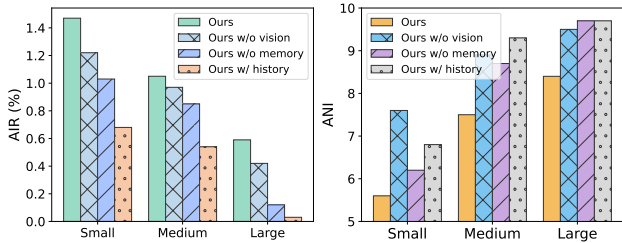


Figure 7: Ablation studies of vision-enhanced evaluation and memory strategies.

consume substantial token budget, introducing noise that may impair decision-making. Overall, the complementary roles of *Eval Agent* and *Memory Agent* significantly enhance system performance: vision-based *Eval Agent* improves evaluation accuracy and supports more meaningful suggestions for improvement, while *Memory Agent* accelerates convergence and enhances robustness.

4.6 Interpretability Analysis (RQ5)

To systematically assess interpretability, we conducted a user study with 10 domain experts in urban sensing, who evaluated the explanations generated during the iterative refinement process. Explanations were rated from 0 to 5 following five dimensions:

- **Clarity:** ease of understanding by humans.
- **Relevance:** direct relation to the improved task solution.
- **Consistency:** alignment with the actual planning behavior.
- **Usefulness:** utility for supporting human decision-making.
- **Granularity:** the level of refinement details.

These criteria assess both linguistic quality and faithfulness to the agent's reasoning and operations.

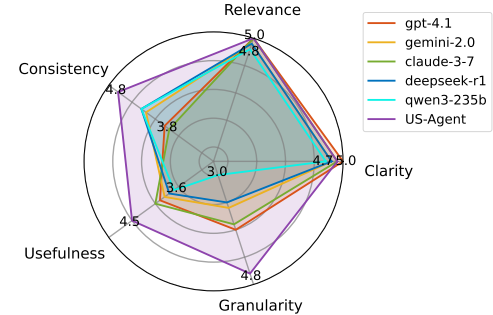


Figure 8: Comparison of interpretability across five dimensions between AgentSense and baseline LLMs.

As shown in Figure 8, AgentSense obtains the highest scores across nearly all five dimensions, consistently surpassing single-agent LLM baselines. Expert evaluations revealed that while GPT-4.1 and Claude-3.7 produced fluent explanations, they occasionally neglected feasibility constraints, leading to lower *Consistency*. Gemini-2.0 favored brevity but often lacked sufficient elaboration, resulting in reduced *Granularity*. Open-source models such as DeepSeek-R1 and Qwen3-235B generated explanations with moderate alignment but limited actionable depth. In contrast, AgentSense's iterative refinement mechanism—linking *Solver Agent* updates with systematic feedback from the *Eval Agent*—produced explanations judged to be both faithful to the underlying operations and sufficiently detailed to support expert reasoning. These findings demonstrate that the multi-agent design enhances not only solution quality but also transparency, yielding explanations that domain experts considered more interpretable, trustworthy, and practically valuable for urban sensing applications.

5 Conclusion and Future Work

In this work, we presented **AgentSense**, a hybrid, training-free framework for web-based participatory urban sensing. By integrating a classical planner with an LLM-driven multi-agent refinement module, AgentSense addresses two central challenges in WPUS: context-aware generalization across heterogeneous and dynamic conditions, and transparent interpretability that elucidates the reasoning behind solution generation. Extensive experiments on two large-scale mobility datasets under varied disturbance settings demonstrate that AgentSense consistently outperforms single-agent LLMs and traditional approaches in both accuracy and adaptability. Expert evaluations further confirm the clarity and reliability of its explanations. Looking forward, we outline two key directions for future work. First, we plan to incorporate geographical attributes of sensing grids to enable personalized path planning, thereby improving efficiency and contextual awareness in task allocation. Second, we aim to enhance scalability by adapting the framework to smaller language models (e.g., 7B or 3B parameters), making AgentSense more resource-efficient and practical for real-world urban sensing deployments.

References

- [1] Zahra Abbasiantaei, Yifei Yuan, Evangelos Kanoulas, and Mohammad Aliannejadi. 2024. Let the llms talk: Simulating human-to-human conversational qa via zero-shot llm-to-llm interactions. In *Proceedings of the 17th ACM International Conference on Web Search and Data Mining*. 8–17.
- [2] Dhruv Agarwal, Srinivasan Iyengar, Manohar Swaminathan, Eash Sharma, Ashish Raj, and Aadithya Hatwar. 2020. Modulo: Drive-by Sensing at City-scale on the Cheap. In *Proceedings of the 3rd ACM SIGCAS Conference on Computing and Sustainable Societies*. 187–197.
- [3] Gati V Aher, Rosa I Arriaga, and Adam Tauman Kalai. 2023. Using large language models to simulate multiple humans and replicate human subject studies. In *International conference on machine learning*. PMLR, 337–371.
- [4] Dimitrios Airantzi, Alice Angus, Gilles Lane, Karen Martin, George Roussos, and Jenson Taylor. 2008. Participatory sensing for urban communities. *UrbanSense08* 11 (2008).
- [5] Lisa P Argyle, Ethan C Busby, Nancy Fulda, Joshua R Gubler, Christopher Rytting, and David Wingate. 2023. Out of one, many: Using language models to simulate human samples. *Political Analysis* 31, 3 (2023), 337–351.
- [6] Henrik Blunck, Niels Olof Bouvin, Tobias Franke, Kaj Grønbæk, Mikkel B Kjaergaard, Paul Lukowicz, and Markus Wüstenberg. 2013. On heterogeneity in mobile sensing applications aiming at representative data collection. In *Proceedings of the 2013 ACM conference on Pervasive and ubiquitous computing adjunct publication*. 1087–1098.
- [7] Lige Ding, Dong Zhao, Mingzhe Cao, and Huadong Ma. 2021. When crowdsourcing meets unmanned vehicles: Toward cost-effective collaborative urban sensing via deep reinforcement learning. *IEEE Internet of Things Journal* 8, 15 (2021), 12150–12162.
- [8] Rong Du, Cailian Chen, Bo Yang, Ning Lu, Xinping Guan, and Xuemin Shen. 2014. Effective urban traffic monitoring by vehicular sensor networks. *IEEE transactions on Vehicular Technology* 64, 1 (2014), 273–286.
- [9] Mohamed Amine Ferrag, Norbert Tihanyi, and Merouane Debbah. 2025. From llm reasoning to autonomous ai agents: A comprehensive review. *arXiv preprint arXiv:2504.19678* (2025).
- [10] Mohammadhossein Ghahramani, MengChu Zhou, and Gang Wang. 2020. Urban sensing based on mobile phone data: Approaches, applications, and challenges. *IEEE/CAA Journal of Automatica Sinica* 7, 3 (2020), 627–637.
- [11] Xusen Guo, Xinxi Yang, Mingxing Peng, Hongliang Lu, Meixin Zhu, and Hai Yang. 2025. Automating traffic model enhancement with AI research agent. *Transportation Research Part C: Emerging Technologies* 178 (2025), 105187.
- [12] Shanshan Han, Qifan Zhang, Yuhang Yao, Weizhao Jin, and Zhaozhuo Xu. 2024. LLM multi-agent systems: Challenges and open problems. *arXiv preprint arXiv:2402.03578* (2024).
- [13] David Hasenfratz, Olga Saukh, Silvan Sturzenegger, Lothar Thiele, et al. 2012. Participatory air pollution monitoring using smartphones. *Mobile Sensing* 1 (2012), 1–5.
- [14] Sirui Hong, Mingchen Zhuge, Jonathan Chen, Xiaiwu Zheng, Yuheng Cheng, Ceyao Zhang, Jinlin Wang, Zili Wang, Steven Ka Shing Yau, Zijuan Lin, et al. 2024. MetaGPT: Meta programming for a multi-agent collaborative framework. International Conference on Learning Representations, ICLR.
- [15] Ce Hou, Fan Zhang, Yong Li, Haifeng Li, Gengchen Mai, Yuhan Kang, Ling Yao, Wenhao Yu, Yao Yao, Song Gao, et al. 2025. Urban sensing in the era of large language models. *The Innovation* 6, 1 (2025).
- [16] Xiaocheng Huang, Yifang Yin, Simon Lim, Guanfeng Wang, Bo Hu, Jagannadan Varadarajan, Shaolin Zheng, Ajay Bulusu, and Roger Zimmermann. 2019. GrabPosisi: An Extensive Real-Life GPS Trajectory Dataset in Southeast Asia. In *Proceedings of the 3rd ACM SIGSPATIAL International Workshop on Prediction of Human Mobility (Chicago, IL, USA) (PredictGIS'19)*. Association for Computing Machinery, New York, NY, USA, 1–10. doi:10.1145/3356995.3364536
- [17] Steffen Hvidt Trier and Tom Jenkins. 2020. Participatory sensing in the speculative smart city. In *Proceedings of the 32nd australian conference on human-computer interaction*. 462–470.
- [18] Shenggong Ji, Yu Zheng, and Tianrui Li. 2016. Urban sensing based on human mobility. In *Proceedings of the 2016 ACM International Joint Conference on Pervasive and Ubiquitous Computing*. 1040–1051.
- [19] Wen Ji, Ke Han, and Tao Liu. 2023. A survey of urban drive-by sensing: An optimization perspective. *Sustainable Cities and Society* 99 (2023), 104874.
- [20] Qijun Jiang, Frank Kresin, Arnold K Bregt, Lammert Kooistra, Emma Pareschi, Edith Van Putten, Hester Volten, and Joost Wesseling. 2016. Citizen sensing for improved urban environmental monitoring. *Journal of Sensors* 2016, 1 (2016), 5656245.
- [21] Zixuan Ke, Fangkai Jiao, Yifei Ming, Xuan-Phi Nguyen, Austin Xu, Do Xuan Long, Minzhi Li, Chengwei Qin, Peifeng Wang, Silvio Savarese, et al. 2025. A survey of frontiers in llm reasoning: Inference scaling, learning to reason, and agentic systems. *arXiv preprint arXiv:2504.09037* (2025).
- [22] Takeshi Kojima, Shixiang Shane Gu, Machel Reid, Yutaka Matsuo, and Yusuke Iwasawa. 2022. Large language models are zero-shot reasoners. *Advances in neural information processing systems* 35 (2022), 22199–22213.
- [23] Feng Li, Wenzhong Shi, and Hua Zhang. 2021. A two-phase clustering approach for urban hotspot detection with spatiotemporal and network constraints. *IEEE Journal of Selected Topics in Applied Earth Observations and Remote Sensing* 14 (2021), 3695–3705.
- [24] Xinyi Li, Sai Wang, Siqi Zeng, Yu Wu, and Yi Yang. 2024. A survey on LLM-based multi-agent systems: workflow, infrastructure, and challenges. *Vicinagearth* 1, 1 (2024), 9.
- [25] Zhonghang Li, Lianghao Xia, Xubin Ren, Jiabin Tang, Tianyi Chen, Yong Xu, and Chao Huang. 2025. Urban Computing in the Era of Large Language Models. *ACM Transactions on Intelligent Systems and Technology* (2025).
- [26] Zhonghang Li, Lianghao Xia, Jiabin Tang, Yong Xu, Lei Shi, Long Xia, Dawei Yin, and Chao Huang. 2024. Urbangpt: Spatio-temporal large language models. In *Proceedings of the 30th ACM SIGKDD Conference on Knowledge Discovery and Data Mining*. 5351–5362.
- [27] Liang Liu, Wu Liu, Yu Zheng, Huadong Ma, and Cheng Zhang. 2018. Third-eye: A mobilephone-enabled crowdsensing system for air quality monitoring. *Proceedings of the ACM on Interactive, Mobile, Wearable and Ubiquitous Technologies* 2, 1 (2018), 1–26.
- [28] Yuhang Liu, Yingxue Zhang, Xin Zhang, Ling Tian, Yanhua Li, and Jun Luo. 2025. UrbanMind: Urban Dynamics Prediction with Multifaceted Spatial-Temporal Large Language Models. In *Proceedings of the 31st ACM SIGKDD Conference on Knowledge Discovery and Data Mining* V. 2. 1951–1962.
- [29] Suhas Mathur, Tong Jin, Nikhil Kasturirangan, Janani Chandrasekaran, Wenzhi Xue, Marco Gruteser, and Wade Trappe. 2010. Parknet: drive-by sensing of roadside parking statistics. In *Proceedings of the 8th international conference on Mobile systems, applications, and services*. 123–136.
- [30] Robin Wentao Ouyang, Animesh Srivastava, Prithvi Prabahar, Romit Roy Choudhury, Merideth Addicott, and F Joseph McClernon. 2013. If you see something, swipe towards it: crowdsourced event localization using smartphones. In *Proceedings of the 2013 ACM international joint conference on Pervasive and ubiquitous computing*. 23–32.
- [31] Mingxing Peng, Yuting Xie, Xusen Guo, Ruoyu Yao, Hai Yang, and Jun Ma. 2025. Ld-scene: Llm-guided diffusion for controllable generation of adversarial safety-critical driving scenarios. *arXiv preprint arXiv:2505.11247* (2025).
- [32] Yiwei Qin, Kaiqiang Song, Yebowen Hu, Wenlin Yao, Sangwoo Cho, Xiaoyang Wang, Xuansheng Wu, Fei Liu, Pengfei Liu, and Dong Yu. 2024. Infobench: Evaluating instruction following ability in large language models. *arXiv preprint arXiv:2401.03601* (2024).
- [33] Mina Sakamura, Tomotaka Ito, Hideyuki Tokuda, Takuro Yonezawa, and Jin Nakazawa. 2015. Minaqn: web-based participatory sensing platform for citizen-centric urban development. In *Adjunct Proceedings of the 2015 ACM International Joint Conference on Pervasive and Ubiquitous Computing and Proceedings of the 2015 ACM International Symposium on Wearable Computers*. 1607–1614.
- [34] Thiago H Silva, Pedro OS Vaz De Melo, Jussara M Almeida, and Antonio AF Loureiro. 2013. Challenges and opportunities on the large scale study of city dynamics using participatory sensing. In *2013 IEEE Symposium on Computers and Communications (ISCC)*. IEEE, 000528–000534.
- [35] Thiago H Silva, Pedro OS Vaz De Melo, Jussara M Almeida, and Antonio AF Loureiro. 2014. Large-scale study of city dynamics and urban social behavior

using participatory sensing. *IEEE Wireless Communications* 21, 1 (2014), 42–51.

[36] Róbert Szabó, Károly Farkas, Márton Ispány, András A Benczúr, Norbert Bátfa, Péter Jeszenszky, Sándor Laki, Anikó Vágner, Lajos Kollár, Cs Sidló, et al. 2013. Framework for smart city applications based on participatory sensing. In *2013 IEEE 4th International Conference on Cognitive Infocommunications (CogInfoCom)*. IEEE, 295–300.

[37] Yashar Talebirad and Amirhossein Nadiri. 2023. Multi-agent collaboration: Harnessing the power of intelligent llm agents. *arXiv preprint arXiv:2306.03314* (2023).

[38] En Wang, Weiting Liu, Wenbin Liu, Yongjian Yang, Bo Yang, and Jie Wu. 2022. Spatiotemporal urban inference and prediction in sparse mobile crowdsensing: A graph neural network approach. *IEEE Transactions on Mobile Computing* 22, 11 (2022), 6784–6799.

[39] Hengzhi Wang, En Wang, Yongjian Yang, Jie Wu, and Falko Dressler. 2022. Privacy-preserving online task assignment in spatial crowdsourcing: A graph-based approach. In *IEEE INFOCOM 2022-IEEE Conference on Computer Communications*. IEEE, 570–579.

[40] Jiawei Wang, Renhe Jiang, Chuang Yang, Zengqing Wu, Makoto Onizuka, Ryosuke Shibasaki, Noboru Koshizuka, and Chuan Xiao. 2024. Large language models as urban residents: An llm agent framework for personal mobility generation. *Advances in Neural Information Processing Systems* 37 (2024), 124547–124574.

[41] Shuliang Wang, Song Tang, Sijie Ruan, Cheng Long, Yuxuan Liang, Qi Li, Ziqiang Yuan, Jie Bao, and Yu Zheng. 2024. Urban Sensing for Multi-Destination Workers via Deep Reinforcement Learning. In *2024 IEEE 40th International Conference on Data Engineering (ICDE)*. IEEE, 4167–4179.

[42] Xiaojie Wang, Zhaolong Ning, Xiping Hu, Edith C-H Ngai, Lei Wang, Bin Hu, and Ricky YK Kwok. 2018. A city-wide real-time traffic management system: Enabling crowdsensing in social Internet of vehicles. *IEEE Communications Magazine* 56, 9 (2018), 19–25.

[43] Zhiheng Xi, Wenxiang Chen, Xin Guo, Wei He, Yiwen Ding, Boyang Hong, Ming Zhang, Junzhe Wang, Senjie Jin, Enyu Zhou, et al. 2025. The rise and potential of large language model based agents: A survey. *Science China Information Sciences* 68, 2 (2025), 121101.

[44] Zelong Xia, Hao Li, Yuehong Chen, and Weisheng Liao. 2019. Identify and delineate urban hotspot areas using a network-based spatiotemporal field clustering method. *ISPRS International Journal of Geo-Information* 8, 8 (2019), 344.

[45] Xiangxiang Xu, Pei Zhang, and Lin Zhang. 2014. Gotcha: a mobile urban sensing system. In *Proceedings of the 12th ACM Conference on Embedded Network Sensor Systems*. 316–317.

[46] Yuwei Yan, Qingbin Zeng, Zhiheng Zheng, Jingzhe Yuan, Jie Feng, Jun Zhang, Fengli Xu, and Yong Li. 2024. Opencity: A scalable platform to simulate urban activities with massive llm agents. *arXiv preprint arXiv:2410.21286* (2024).

[47] Xiaojun X Yang. 2021. *Urban remote sensing: monitoring, synthesis and modeling in the urban environment*. John Wiley & Sons.

[48] Jing Yuan, Yu Zheng, Chengyang Zhang, Wenlei Xie, Xing Xie, Guangzhong Sun, and Yan Huang. 2010. T-drive: driving directions based on taxi trajectories. In *Proceedings of the 18th SIGSPATIAL International Conference on Advances in Geographic Information Systems (San Jose, California) (GIS '10)*. Association for Computing Machinery, New York, NY, USA, 99–108. [doi:10.1145/1869790.1869807](https://doi.org/10.1145/1869790.1869807)

[49] Zhiyuau Zeng, Jiatong Yu, Tianyu Gao, Yu Meng, Tanya Goyal, and Danqi Chen. 2023. Evaluating large language models at evaluating instruction following. *arXiv preprint arXiv:2310.07641* (2023).

[50] Yang Zhang, Lanyu Shang, Ruohan Zong, Zeng Wang, Ziyi Kou, and Dong Wang. 2021. StreamCollab: A streaming crowd-AI collaborative system to smart urban infrastructure monitoring in social sensing. In *Proceedings of the AAAI Conference on Human Computation and Crowdsourcing*, Vol. 9. 179–190.

[51] Yang Zhang, Shixin Yang, Chenjia Bai, Fei Wu, Xiu Li, Zhen Wang, and Xuelong Li. 2024. Towards efficient llm grounding for embodied multi-agent collaboration. *arXiv preprint arXiv:2405.14314* (2024).

[52] Xuefeng Zhao, Niannian Wang, Ruicong Han, Botao Xie, Yan Yu, Mingchu Li, and Jinping Ou. 2018. Urban infrastructure safety system based on mobile crowdsensing. *International journal of disaster risk reduction* 27 (2018), 427–438.

[53] Yu Zheng, Tong Liu, Yilun Wang, Yanmin Zhu, Yanchi Liu, and Eric Chang. 2014. Diagnosing New York city's noises with ubiquitous data. In *Proceedings of the 2014 ACM international joint conference on pervasive and ubiquitous computing*. 715–725.

[54] Zhilun Zhou, Yuming Lin, Depeng Jin, and Yong Li. 2024. Large language model for participatory urban planning. *arXiv preprint arXiv:2402.17161* (2024).

[55] Xingchen Zou, Yibo Yan, Xixuan Hao, Yuehong Hu, Haomin Wen, Erdong Liu, Junbo Zhang, Yong Li, Tianrui Li, Yu Zheng, et al. 2025. Deep learning for cross-domain data fusion in urban computing: Taxonomy, advances, and outlook. *Information Fusion* 113 (2025), 102606.

Appendix

A Baseline Planner

This appendix summarizes the six baseline planners adopted in our study. All methods produce an initial feasible schedule S_0 that meets budget and temporal constraints before refinement. The first five are reproduced from [41], and the *GraphDP* algorithm follows [18].

- **Random (RN).** For each worker, an initial route is generated from its origin to a fixed destination using the *Nearest Neighbor* heuristic. Sensing tasks are then randomly inserted into feasible positions along the route until the worker's budget is exhausted. This provides a purely stochastic baseline that satisfies route and cost constraints.
- **Task Value Priority Greedy (TVPG).** TVPG starts from the same *Nearest Neighbor* route construction but greedily inserts tasks that yield the highest marginal coverage gain when added to any feasible position of a worker's route. When multiple tasks offer equal gain, the task with the lower incentive cost is selected.
- **Task Cost Priority Greedy (TCPG).** Similar to TVPG, TCPG also evaluates feasible insertions but prioritizes tasks with lower incentive costs. If several tasks share the same cost, the one that provides higher coverage gain is preferred.
- **Multi-Start Simulated Annealing (MSA).** MSA performs iterative local search over complete worker routes through random operations such as swapping, insertion, and reversal. Each candidate modification must preserve route feasibility (budget and connectivity). Multiple random restarts are executed to escape local minima and improve robustness.
- **Multi-Start Simulated Annealing with Greedy Initialization (MSAGI).** MSAGI enhances MSA by initializing each run with the greedy solution from TVPG instead of random routes. This improves convergence speed and solution quality by combining heuristic initialization with metaheuristic search.
- **Graph-based Dynamic Programming (GraphDP).** GraphDP constructs a time-layered location graph for each worker and applies dynamic programming to search near-optimal paths that maximize spatial-temporal coverage based on marginal entropy gains. Then worker replacement further improves overall coverage by swapping low-contribution workers with better candidates until no significant gain is achieved.

B System Prompts

This section presents the complete prompt designs used for the three core agents in the *AgentSense* framework. Each prompt defines the agent's role and goal, input structure, and the output format. Specifically, Section B.1 details the *Solver Agent* prompt that guides solution generation and modification; Section B.2 describes the *Eval Agent* prompt for assessing solution quality and constraint compliance; and Section B.3 provides the *Memory Agent* prompt used to retrieve and reuse prior meta-operations for experience-aware refinement.

B.1 Solver Agent Prompt

Role and Goal:

You are an expert in solving the urban sensing task assignment problem. Your goal is to improve a baseline solution according to the given instructions while ensuring compliance with budget and feasibility constraints.

Inputs:

You will be given the following information for your task:

- **Task settings:** global information of the task, such as grid size, total budget and task time range.
- **Worker info:** information of the worker candidates, such as origin, destination, time windows, and speed.
- **Baseline solution:** task assignments from baseline planner.
- **Instructions:** "continue optimize" or one of [disturbance types].

Constraints:

You need to consider the following constraints:

- Worker must start/end at origin/dest within time window.
- Worker move in four direction: up, down, left, right, or stay.
- Total cost should be within the total budget.

Tools you can use:

- `validate_worker_paths`
 parameters: {"worker_paths": [...], "worker_infos": [...], ...}.
 return: {"overall_feasible": bool, "validation_results": ...}.

Final output:

Organize your final answer as following:

- **think_process:** up to 200 words summary of reasoning process.
- **refined_solution:** {"worker_id": [[x, y, t], [x, y, t], ...], ...} .

B.2 Eval Agent prompt

Role and Goal:

You are an expert in urban sensing task allocation. Given a candidate solution, your task is to evaluate its performance using quantitative metrics and visual evidence, and then provide clear, specific, and actionable recommendations for improvement.

Inputs:

The baseline and refined solutions in the following format:

- {"worker_id": [[x, y, t], [x, y, t], ...], ...}. A dictionary where each key is a worker ID, and the value is a list of grid positions [x, y, t] representing the worker's assigned trajectory over space and time.

Instruction:

- Use tools to check how well the solution handles disturbances.
- Use tools to compute the objective value and cost of the solution.
- Use tools to generate a visualization that compares the refined solution with the baseline.
- When providing suggestions, base them on both the quantitative evaluation and the visual evidence.

Tools you can use:

- `check_disturbance_handling(...)`
 - `compute_objective(...)`
 - `compute_cost(...)`
 - `visual_analysis(...)`

Final output:

Organize your final answer as following:

- **eval_summary:** a concise summary of the evaluation results.
- **advice:** specific, actionable advice for improving the solution.

B.3 Memory Agent prompt

Role and Goal:

You are a memory manager in urban sensing task allocation. Your goal is to detect differences between baseline and refined solutions, extract the most critical adaptation as a *meta-operation*, and store it in memory so that the system can leverage this knowledge to improve future urban sensing solutions.

Inputs:

You will be provided with the baseline and refined solutions along with their evaluation metrics in the following format:

- **Solution:** `{"worker_id": [[x, y, t], [x, y, t], ...], ...}`. A dictionary where each key is a worker ID, and the value is a list of grid positions $[x, y, t]$ representing the worker's assigned trajectory over space and time.

- **Metrics:** `covered_count, entropy, objective_value, cost`.

Instruction:

- Operation types: `add_worker, remove_worker, modify_path, other`.
- First, detect all differences between baseline and refined solutions.
- Next, determine the most significant difference.
- Finally, combine this difference with the changes observed in the metrics to produce the output.

Final output:

Organize your final answer as following:

- **operation_type:** the category of the difference between solutions.
- **operation_details:** a concise description of what changed and how it affected the metrics.

C More Experimental Results for Temperature

We also evaluate AgentSense with different base LLMs and analyze the impact of decoding temperature. As shown in Figure 9, the optimal temperature varies across models. GPT-4.1 achieves its highest AIR (1.10%) at $T = 0.5$, while Gemini-2.0-Flash performs best at $T = 0.1$, suggesting that more deterministic decoding improves stability. Claude-3-7-Sonnet benefits from moderate exploration, reaching 2.33% AIR at $T = 0.5$, but its performance declines at $T = 0.9$, indicating that excessive randomness reduces robustness. In contrast, open-source models such as Qwen3 and Llama-3 remain relatively stable across all temperatures. Moreover, the ANI metric reveals that lower temperatures generally lead to faster convergence, as fewer iterations are required to reach valid improvements. Overall, these results highlight two key insights: (i) AgentSense is compatible with both proprietary and open-source LLMs, consistently enforcing budget feasibility across all settings, and (ii) careful tuning of decoding temperature is essential to balance exploration and exploitation, as different LLMs exhibit distinct sensitivities to sampling variability.

D More Results for Disturbance Adaptation

Figure 10 presents five representative types of disturbances considered in this study: *budget change*, *bad weather*, *worker unavailable*, *area blocked*, and *mid-path visiting*. These cases illustrate how AgentSense adapts to diverse real-world disturbances through interpretable reasoning and adaptive replanning. In the T-Drive *Small* setting, AgentSense responds to budget rising by adding workers while avoiding redundant routes, reorganizes trajectories under bad weather to account for slower movement, and reassigns coverage when a worker becomes unavailable. In the Grab-Posisi *Medium* setting, it reroutes affected paths to bypass a blocked area and adjusts trajectories to fulfill new mid-path visiting requests without

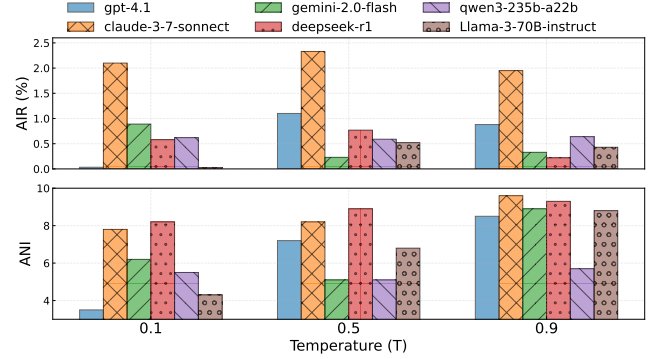


Figure 9: Comparison of different base LLMs within AgentSense under varying temperature settings in the T-Drive Medium configuration.

violating constraints. Across all scenarios, AgentSense maintains feasible, high-coverage solutions and provides clear reasoning for each refinement step, highlighting its robustness and interpretability under dynamic urban conditions.

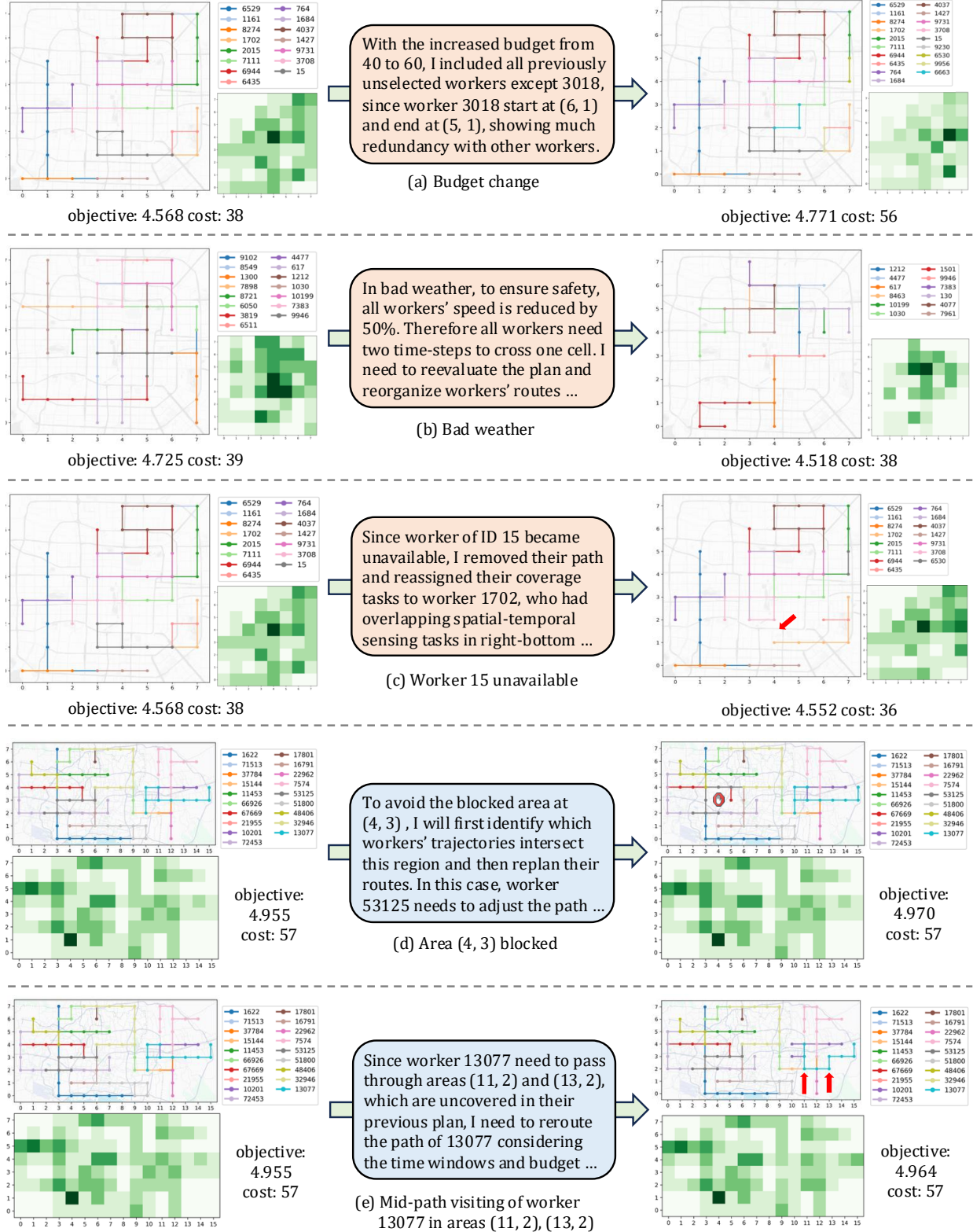


Figure 10: Visualization and reasoning results of AgentSense under different types of disturbances. The first three cases are from the T-Drive *Small* setting, and the last two are from the Grab-Posisi *Medium* setting.